AMERICAN ACADEMY OF OPHTHALMOLOGY®

Retromode Imaging Technology for Detecting Drusen-Like Deposits in Healthy Adults

Mariano Cozzi, MSc,[1] *Davide Monteduro, MD,*[1] *Matteo Airaldi, MD,*[1] *Salvatore Parrulli, MD,*[1] *Federico Cinus, MD,*[1] *Andrea Trinco, MD,*[1] *Giovanni Staurenghi, MD,*[1] *Alessandro Invernizzi, MD*[1,2]

Purpose: To investigate the ability of retromode imaging technology to visualize drusen-like deposits (DLDs) in the macular region of healthy individuals without retinal diseases. Additionally, the correlation between subject age and the density of DLDs was assessed and their topographic distribution was evaluated.

Design: Prospective, observational, cross-sectional study

Subjects: Healthy volunteers (aged $\geq$ 35 years) without macular diseases.

Methods: This study evaluated macular images in healthy adults using color fundus photography (FP) and retromode imaging. Two masked graders counted the number of DLDs identifiable with each modality. The standardized ETDRS concentric rings were adopted to divide DLDs based on their topographic distribution.

Main Outcome Measures: Comparison of the number of DLDs detected with each imaging modality. The association between DLDs and age. The topographic distribution of macular DLDs with retromode imaging.

Results: The study included 91 eyes of 52 healthy volunteers (mean $\pm$ standard deviation age, 57.9 $\pm$ 10.9 years; range, 36–82 years). Overall, at least 1 DLD was present in 63.74% of eyes on color FP and 96.71% on retromode. Retromode imaging allowed detection of significantly more DLDs compared with color FP within the ETDRS grid (median [interquartile range], 4 [1–14] vs. 0 [0–0] respectively; $P < 0.001$). The density of DLDs was higher in the outer and inner rings compared with the central subfield (relative risk [RR], 16.70; 95% confidence interval [CI], 10.3–27.3 vs. RR 17.1; 95% CI, 10.5–27.6, respectively). Age was significantly correlated with DLDs density in all 3 sectors (all $P < 0.05$).

Conclusions: Retromode technology allowed the detection of a significantly higher number of DLDs compared with FP in the macula of healthy individuals. This noninvasive imaging modality could be used to investigate the effect of the aging process on the macula, fostering a better understanding of the pathophysiology of age-related macular diseases.

Financial Disclosure(s): Proprietary or commercial disclosure may be found in the Footnotes and Disclosures at the end of this article. *Ophthalmology Retina 2023;7:1051-1058 © 2023 by the American Academy of Ophthalmology. This is an open access article under the CC BY license (http://creativecommons.org/licenses/by/4.0/).*

Age-related macular degeneration (AMD) by definition affects subjects aged > 55 years. However, the reason why some individuals develop an age-related disease remains unclear, and it can not only be ascribed to the aging process.[1]

The presence of drusen is the initial sign and hallmark of AMD. These lesions are represented by the accumulation of extracellular debris between the inner collagenous layer of Bruch's membrane (BM) and the basal lamina of the retinal pigment epithelium (RPE).[2]

On ophthalmoscopy, yellow–white dots with sharply defined borders and a diameter of < 63 μm are generally referred to as small hard drusen, or "drupelets."[3,4] They are considered a normal consequence of aging. However, there is a subtle progression from drupelets to drusen, marking the shift from a physiologic aging process to a diagnosis of AMD.[5] Other age-related retinal changes include, increased thickness of BM,[6] lipid accumulation,[7] and thinning of different retinal layers.[8]

Detection of the early signs of AMD is considered crucial for planning patient follow-up, monitoring disease progression, and, possibly, offering treatments currently under investigation. Although the AMD classification is still based on color fundus photography (FP), more recent imaging modalities such as spectral-domain OCT (SD-OCT) have demonstrated better assessment of the changes affecting retinal layers because of AMD. In this context, retromode modality is an emerging imaging technology that is extremely reliable in identifying and classifying different kinds of drusen and drusenlike deposits (DLDs), including particularly small lesions.[9]

The purpose of this study was to investigate the ability of retromode technology to identify the presence of DLDs in a pool of healthy adults without macular disease, describe their topographic distribution, and test for correlations between their quantity and subject age.

https://doi.org/10.1016/j.oret.2023.07.012
ISSN 2468-6530/23

Methods

This single-center, observational, cross-sectional study was approved by the Milano Area 1 institutional review board and was conducted in accordance with the tenets of the Declaration of Helsinki. Written informed consent was obtained from all eligible participants at the time of enrollment.

Study Population

Adult volunteers with no reported history of retinal or ocular diseases presenting to the general ophthalmology service at the Eye Clinic, in the Department of Biomedical and Clinical Science, Luigi Sacco Hospital, University of Milan, Milan, Italy, were enrolled in the study. Inclusion criteria were as follows: adults aged $\geq$ 35 years with a spherical equivalent refractive error within $\pm$ 5 diopters (D), normal visual acuity with an ETDRS score of $\geq$ 80 letters, and a healthy self-reported ocular and systemic history. Only adult subjects were included because they were expected to exhibit a higher prevalence of DLDs due to the physiologic aging process. Other inclusion criteria were a routine ophthalmic examination at the time of the study visit that indicated no corneal or media opacities that would preclude fundus imaging and the absence of clear DLDs or any other signs of AMD in either eye. A self-reported questionnaire was used to collect general relevant parameters, such as diabetes, systemic hypertension, dyslipidemia, smoker/nonsmoker, and any oral supplementation therapy.

Procedures

Each subject underwent a comprehensive ophthalmic examination including measurement of best-corrected visual acuity, slit-lamp biomicroscopy, and dilated funduscopy before the imaging session.

All eyes included in the study were imaged with a confocal true-color FP imaging system (Eidon; Centervue) covering 60° of the retina (pupil angle) with the fixation target centered on the fovea and a resolution of 3680 $\times$ 3288 pixels. All eyes were also imaged with near-infrared wavelength (790 nm) retromode illumination (Mirante; Nidek Co. Ltd.) both with the confocal aperture deviated-right (DR) and deviated-left (DL). The resulting monochromatic images (DR or DL) consisted of a single 45° (pupil angle) fundus retromode image centered on the macula with a resolution of 2048 $\times$ 2048 pixels and averaged at least 40 frames. To better emphasize the cross-sectional findings, a new high-resolution OCT Spectralis (Heidelberg Engineering) was also used to scan an area where the retromode image exhibited the presence of small DLDs in a single patient (not part of the study protocol).

Grading Protocol

After image acquisition, the entire set of images was analyzed by 2 independent imaging experts (M.C. and D.M.) in a masked fashion using a standardized protocol. First, each participant was anonymized by a third observer to minimize any diagnostic biases. Eidon color fundus images were exported from the device and imported into ImageJ software (Rasband, WS, ImageJ, US National Institutes of Health, https://imagej.nih.gov/ij/, 1997–2018) for the quantitative assessment and resized to cover the same field of view as the retromode image. Each reviewer counted the number of DLDs (if present) and annotated the location as superior hemifield, inferior hemifield, or any of the 3 rings (center, inner, and outer) of the ETDRS map, which was superimposed on the color image (Fig 1). Drusen-like deposits detected within the ETDRS grid were not counted in the superior or inferior hemifield. The same approach was used with the monochromatic retromode image using the built-in Mirante software (Navis-Ex 1.9.0; Nidek Co., Ltd.). A customized ETDRS grid was implemented by NIDEK and an image registration tool allowed grid centration on the fovea, which is normally not detectable in the purely retromode image. Briefly, the system enables the use of color images from the Mirante to identify the foveal center and automatically coregister the retromode and color images.

Drusen-like deposits on FP were identified as yellowish round deposits,[2] whereas on retromode they were recognized as craters or mounds with a dark shadow on their right or left side.[9] Currently, there is no standardized and universally accepted classification scheme for drusen due to the aging process, hence we were limited to using this generalized characterization.

Statistical Analysis

All statistical analyses were performed using open-source software R version 4.2.1 (R Project; The R Foundation for Statistical Computing). All tests were 2-tailed, and P values of < 0.05 were considered statistically significant.

The distribution of quantitative variables was assessed using the quantile–quantile plot. In this study, variables are reported as mean (standard deviation [SD]), median (interquartile range [IQR]), or number (percentage) as appropriate. The Shapiro–Wilk test was used to determine the distribution of age.

The interrater reliability between the 2 masked readers was calculated using the intraclass correlation coefficient (ICC) for retromode and color FP in all sectors.

A nonparametric Wilcoxon signed-rank test was used to compare the difference in the number of detected DLDs between color photography and retromode.

Poisson generalized linear mixed-effects models (GLMMs) were used to estimate the count and/or density of detected DLDs according to the device and retinal field.

The drusen count was used to compare corresponding areas between the 2 devices. The drusen density (defined as the number of drusen divided by the area of interest) was used to examine the association between drusen load and age across the central, inner, and outer subfields.

The first Poisson GLMMs included an interaction between device type (color vs. retromode) and retinal fields as the main predictor variables.

The second Poisson GLMM included only data originating from retromode imaging. In this model, the main predictor variable was the interaction of retinal subfield and age. When ETRDS subfields were considered, the expected density of DLDs was predicted, accounting for different areas of the concentric ETDRS rings.

All models also included age and gender as fixed effects, as well as a random intercept for eyes within patients as random effects, to account for intrasubject and intersubject variability.

Results

Overall, 110 potential eyes fulfilling the inclusion criteria were screened and imaged at the Eye Clinic at Luigi Sacco Hospital, University of Milan. Among these, 91 eyes from 52 healthy volunteers were eligible for analysis as the remaining 19 eyes had at least 1 low-quality image that warranted exclusion. The age range of the study sample was normally distributed (Shapiro–Wilk W, 0.98; $P = 0.187$). The mean age of the study sample was 57.9 $\pm$ 10.9 years (range, 36–82 years). Table 1 presents the characteristics of the study sample.

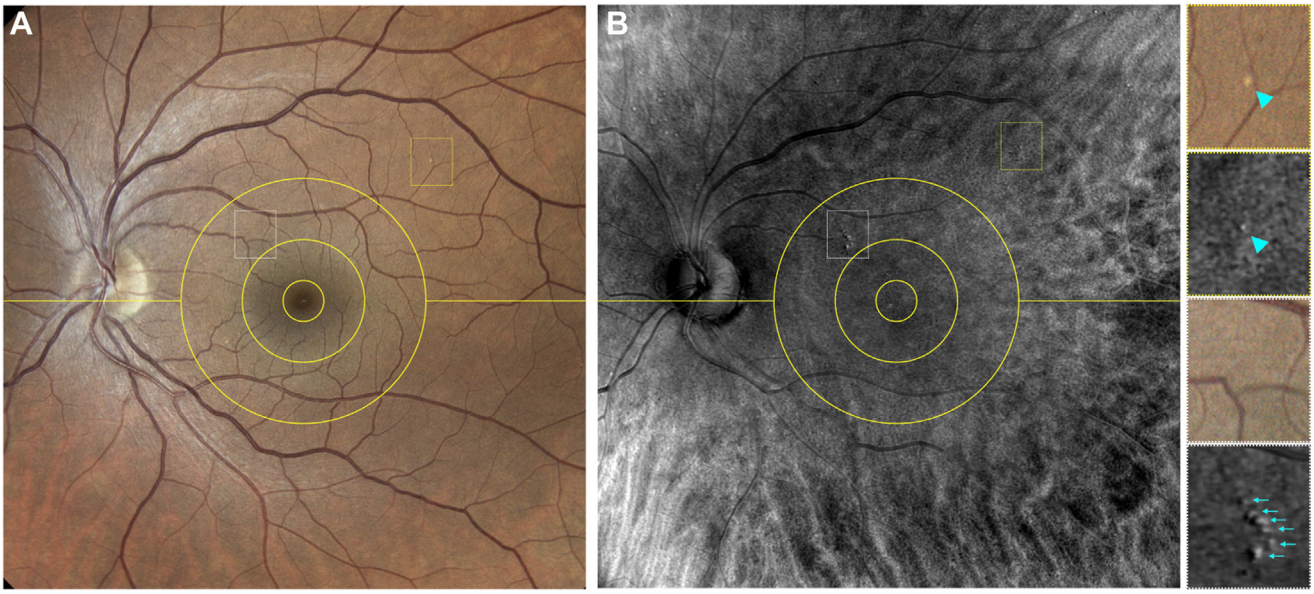

Figure 1. Cropped 45° true-color Eidon fundus photography (**A**) compared with 45° retromode fundus image (**B**) of a 51-year-old healthy volunteer. The 3 ETDRS concentric rings were superimposed to exactly measure the drusen-like deposits (DLDs) count in the macular area. The yellow-dotted magnified square reveals a single druse visible with both technologies. Conversely, the white-dotted magnified frame highlights absence of alterations on color fundus photography, whereas there are 6 clearly visible DLDs in the outer ETDRS ring on the retromode.

The agreement between readers for FP and retromode was good in the 3 ETDRS sectors (all ICCs > 0.85; 95% CI, 0.83−0.92). There was moderate agreement in the superior and inferior hemifields for FP (ICC, 0.73; 95% CI, 0.66−0.81) and retromode (ICC, 0.77; 95% CI, 0.68−0.83). As the interrater reliability was considered high in all sectors, the following analyses were performed based on grader 1 data (M.C.).

Retromode vs. Color Photography

Overall, 63.74% of eyes exhibited at least 1 druse on FP and 96.71% on retromode. Among the included eyes, 19.78% exhibited at least 1 DLD on color FP within the ETDRS grid area, whereas 82.42% of eyes had at least 1 DLD on retromode imaging.

Table 1. Demographic Characteristics

Number of eyes	91
Number of subjects	52
Age, yrs, mean (SD)	57.9 (10.9)
Female, n (%)	34 (64.6)
Male, n (%)	18 (35.6)
Laterality OD, n (%)	47 (51.6)
Laterality OS, n (%)	44 (48.4)
Systemic variables	
Type 2 diabetes, n (%)	1 (1.9)
Hypertension, n (%)	11 (21.1)
Dyslipidemia, n (%)	14 (26.9)
Smoking status	
Current every day smoker, n (%)	6 (11.5)
Current, weekly smoker, n (%)	5 (9.6)
Former smoker, n (%)	17 (32.7)
Never smoker, n (%)	24 (46.2)

OD = right eye; OS = left eye; SD = standard deviation.
Data are mean (SD) or n (%).

The retromode modality enabled detection of a significantly larger number of DLDs in all sectors and fields evaluated in this study compared with FP (Table 2; $P < 0.001$, all comparisons). The median (IQR) count of DLDs in the entire ETDRS grid was 4 (1−14) for retromode and 0 (0−0) with color FP in the same area (Table 2; $P < 0.001$). In the superior hemiretina, the median was 11 DLDs (IQR, 5−33) detected with retromode and 0 DLDs (IQR, 0−2) detected with color FP (Table 2; $P < 0.001$). In the inferior hemiretina the median was 14 DLDs (IQR, 4−27) detected with retromode and 0 DLDs (IQR, 0−1) detected with color FP (Table 2; $P < 0.001$). Figure 2 summarizes the statistically significant differences between imaging modalities in all fields.

Retromode Detected DLDs and Age

The analysis of each of the 3 concentric ETDRS rings on retromode imaging indicated that DLD density was higher in the outer and inner rings compared with the central ring. The expected DLDs density in the outer ring was 16.70 times that in the central segment (relative risk [RR], 16.70; 95% confidence interval [CI], 10.3−27.3] whereas the expected DLDs density in the inner ring was 17.1 times that of the central circle (RR, 17.1; 95% CI, 10.5−27.6; Fig 3).

The RR of detecting DLDs in the inferior hemiretina and superior hemiretina was similar (RR, 0.89; 95% CI, 0.74−1.08).

The overall DLD density increased by 5% per year (RR, 1.05; 95% CI, 1.01−1.09). Age was statistically significantly correlated with DLD density in all 3 ETDRS sectors (concentric rings, $P = 0.003$).

Discussion

Drusen-like deposits commonly occur with aging, and they are considered the hallmark of age-related macular

Table 2. Comparison of the Drusen Count and Drusen Expected Count between Color Fundus Photography and Retromode Imaging

	Drusen Observed Count					Drusen Expected Count				
	Color		Retromode			Color		Retromode		
	Median	IQR	Median	IQR	P Value	Count	95% CI	Count	95% CI	P Value
ETDRS rings										
Outer	0	0–0	3	1–8	< 0.001	0.10	0.06–0.18	2.17	1.37–3.43	< 0.001
Inner	0	0–0	0	0–2.5	< 0.001	0.04	0.02–0.10	0.92	0.57–1.47	< 0.001
Center	0	0–0	0	0–0	< 0.001	0.03	0.01–0.08	0.18	0.11–0.32	< 0.001
ETDRS total	0	0–0	4	1–14	< 0.001	0.16	0.09–0.28	3.28	2.08–5.16	< 0.001
Hemiretina										
Superior	0	0–2	11	5–33	< 0.001	0.98	0.71–1.37	12.67	9.46–16.96	< 0.001
Inferior	0	0–1	14	4–27	< 0.001	1.17	0.84–1.61	10.84	8.01–14.52	< 0.001
Total	1	0–3	28	11–63	< 0.001	2.15	1.58–2.92	23.50	17.58–31.42	< 0.001

CI = confidence interval; IQR = interquartile range.

generation. However, several drusen classifications have been proposed based on their appearance and clinical relevance. For instance, small drusen/DLDs are now considered part of the normal aging and were the only type investigated in this study. We found that retromode technology allowed detection of a larger number of DLDs than conventional color FP in healthy adults. These DLDs are clearly not related to a pathologic condition because they significantly increase in a manner consistent with the physiologic process of aging. This aging process initially affects the outer ETDRS rings, whereas the central circle remains mostly absent of DLDs.

Recent studies of retromode imaging evaluated different drusen phenotypes along with other imaging modalities in sample of patients with clinically confirmed early or intermediate AMD.[9,10] Our group first implemented the Mirante retromode modality as part of multimodal imaging for the characterization of drusen subtypes. In fact, we found that retromode technology allowed us to detect many more

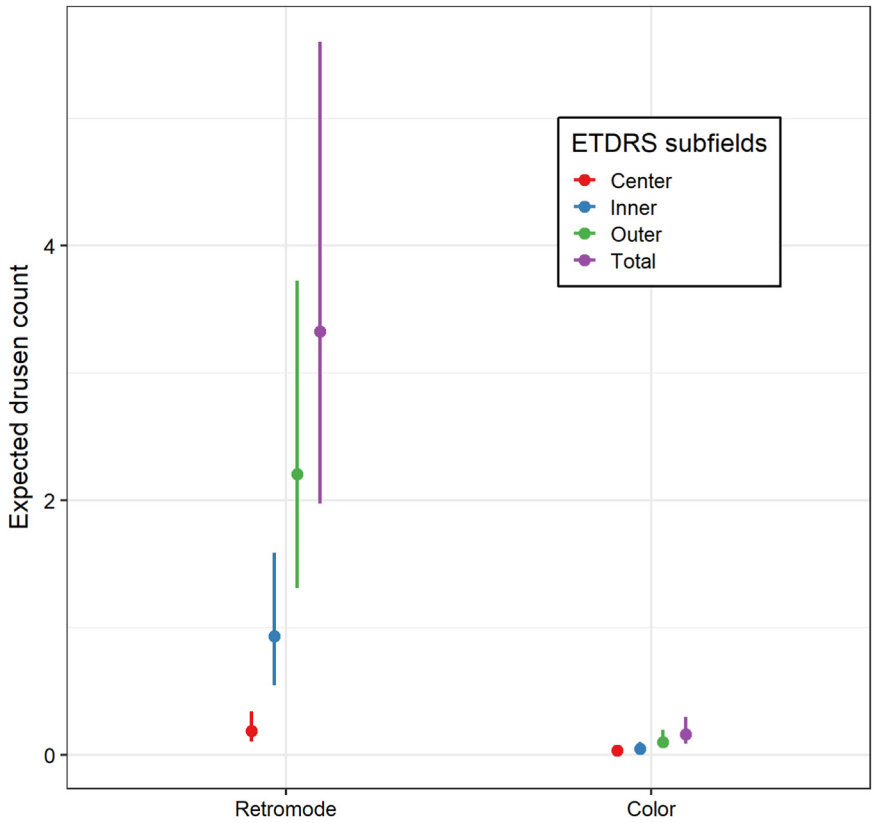

Figure 2. Graphic representation of the drusen-like deposits (DLDs) expected count in the 3 ETDRS concentric rings obtained by the Poisson generalized linear model between color photography and retromode. The figure shows the medians and the 95% confidential intervals of DLDs expected count.

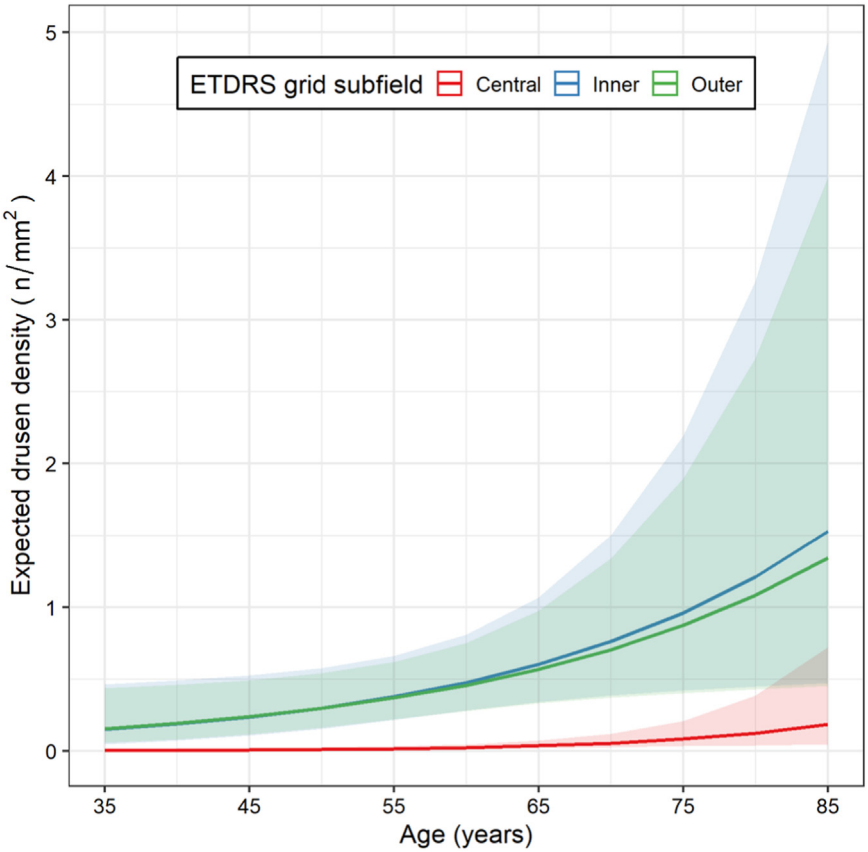

Figure 3. Visual representation of the expected drusen-like deposits (DLDs) density expressed as the number of DLDs per millimeter square in the 3 ETDRS concentric rings compared with the age detected on retromode. The graph clearly emphasizes the difference in the DLDs density between the inner and outer rings compared with the central millimeter ETDRS subfield. Age was found to be correlated with the DLDs density in all ETDRS sectors ($P = 0.003$).

small or medium (< 125 μm) drusen with higher sensitivity than other imaging modalities.[11] The results from the present study further confirm the ability of retromode to visualize extremely tiny RPE elevations not detectable by FP.

Previous studies on patients with AMD compared retromode technology and flash-based FP using a different device (F-10 SLO; NIDEK Co. Ltd.). These studies first demonstrated the capability of retromode to monitor subtle changes in non-advanced AMD.[12,13] In fact, even in eyes affected by AMD, drusen were more easily visualized with the retromode technology (the F-10 device had a lower resolution without the possibility to average multiple frames). A reason for the greater performance of retromode could be due to the unique technology and imaging principle. Briefly, the lateral incident light generates a shadow on the opposite side of the pathology, enhancing the contrast of RPE elevations. Measurement of DLD size is not possible with retromode because the anatomy that contributes to generate the DLD signal is also the projected shadow on the image; thus, the measure would be overestimated.

In this study, we quantified DLDs density seen on retromode in 3 different concentric ETDRS rings. We found that density was notably higher in the outer and inner rings, whereas the center ring had the lowest density. This distribution is consistent with histopathologic studies of AMD. In fact, there is evidence that photoreceptor degeneration occurs earlier in rods, which are mainly present outside the fovea, than in cones.[14] Functional tests also confirmed this hypothesis in which rods are at risk of degeneration in both aging and AMD.[15–18] As functional tests, such as dark adaptation, are currently considered a biomarker for early AMD and macular aging, retromode imaging might be a complementary anatomic test for detecting extremely early changes in the macular region. Notably, the spatial distribution of drusen in patients with intermediate AMD exhibits an opposite pattern. Multiple studies have demonstrated a greater abundance of drusen in the central ETDRS subfield due to the higher cone density.[19–22] A recent MACUSTAR report further confirmed the greater abundance in the foveal area.[23] However, they presented the topographic distribution of drusen in subjects with early AMD similar to our findings.[23] A possible explanation is that the higher drusen load in the outer ETDRS fields is a normal consequence of aging, whereas the mechanism seems to be inverted in the intermediate form of the disease. Clinically, these insights on age and location of pathology may aid in disease staging and prognostication.

Drusen can be present in the young adult population.[24–26] For example, Silvestri et al[26] used FP and reported a drusen prevalence of 91.48 % of gradable eyes

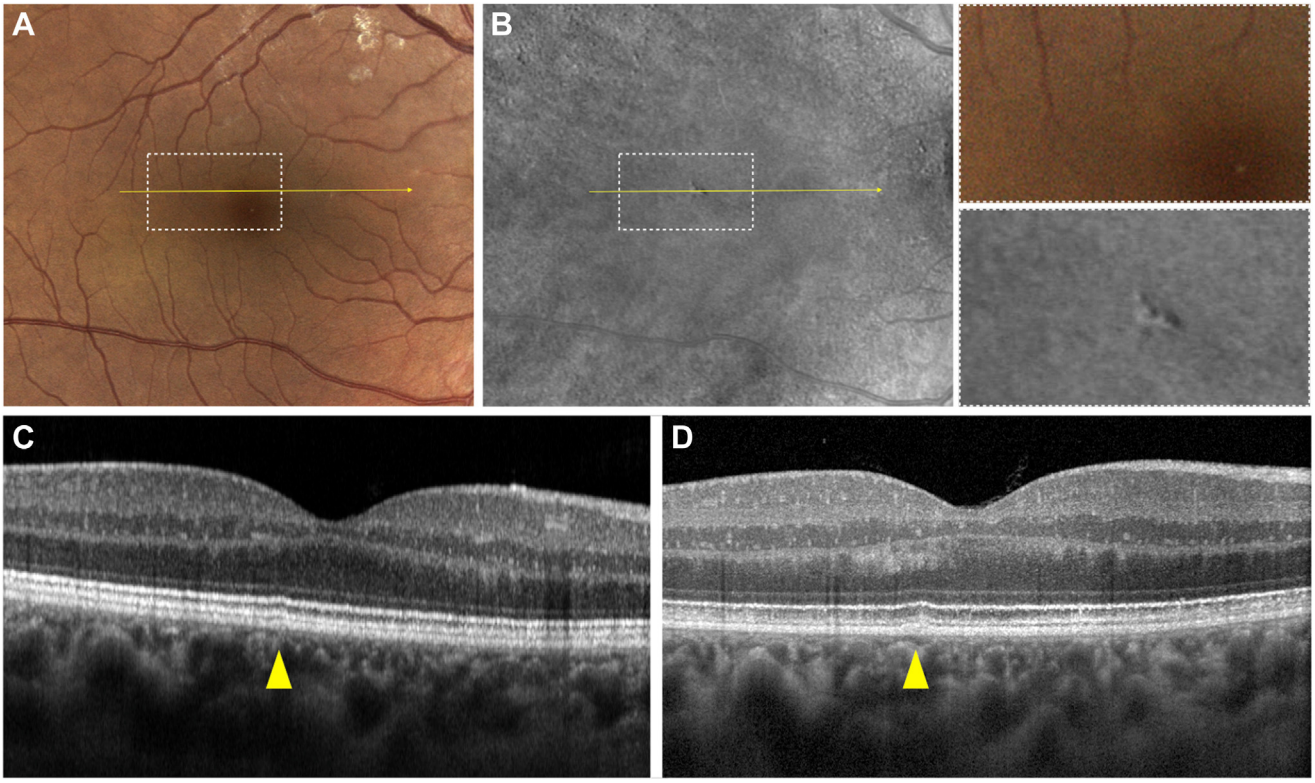

Figure 4. Representative case of a healthy patient imaged with both (**A**) color fundus photography and (**B**) retromode technology. The magnified frames clearly exhibit the discordance between the 2 technologies to show retinal pigment epithelium (RPE) alterations at the posterior pole. (**C**) Conventional spectral-domain OCT barely shows a small RPE elevation defined by the yellow arrowhead. (**D**) The same section scanned with the high-resolution research platform reveals a small sub-RPE deposit with the consequent remodeling of the above hyperreflective layers.

in a White population aged 18 to 54 years. They also found the drusen load increased with increasing age.[24] Previous studies have described the presence of drusen in 94% of healthy adults,[24,27] which has been further confirmed in a clinicopathologic study.[25] A study of young healthy adults reported small, hard drusen on color photographs in 21 of 97 participants.[28] Data on macular drusen in healthy children were also published, showing the presence of drusen in 11% of participants aged 11 to 12 years.[29] These studies corroborate the assumption that drusen might be present in most healthy subjects without necessarily being a harbinger of pathology. However, none of these findings investigated the macular topographic distribution of drusen. In the current study, DLDs were present at the posterior pole in young healthy adults aged $\geq$ 35 years. Although our findings indicate that retromode imaging was superior, conventional color FP was able to identify some DLDs.

In our experience DLDs have a characteristic appearance on retromode imaging. To the best of our knowledge, there are no confounding factors that mimic this appearance on retromode imaging. Ideally, a correlation between retromode imaging and OCT would beneficial. However, retromode–OCT correlation was not part of the study design because point-by-point anatomic correlation between modalities is not possible. Despite being extremely useful to characterize the drusen phenotype, OCT volume is not an adequate approach for detecting the presence of small drusen and DLDs. A dedicated customized dense OCT scan confirmed the previous correlations between what is visualized on retromode and other imaging modalities[9,30] (Fig 4). Conventional SD-OCT has an axial resolution of approximately 7 μm and a lateral resolution of 14 μm, which is often insufficient to discriminate the small RPE elevations investigated in this study. Newer high-resolution OCT, with an axial resolution of 3 μm in tissue, may provide novel insights, differentiating the presence of 2 closely spaced points in the RPE layer.[31,32]

There are some limitations to this study including the cross-sectional design of the protocol. In fact, the application of the retromode technology in a long-term, prospective study would better characterize the changes in DLDs over time. Additionally, the retromode imaging principle precludes measurement of DLD size. An empirically validated approach would help in the comparison of different technologies. An investigation of the distribution of DLDs based on systemic factors (e.g., diabetes) was not the primary aim of this study and, therefore, was not evaluated here. Furthermore, the small number of individuals with systemic factors precluded statistical analysis. Lastly, the system does not allow simultaneous imaging of OCT scans with retromode modality because the enface imaging barely displays retinal vessels and the tracking system would not be able to compensate. A point-by-point correlation between OCT and

retromode on the same device would add more insights between structural signs and topographic localization. Perhaps the incorporation of higher resolution OCT may aid in the understanding of DLD development.

In conclusion, the density of DLDs in a cohort of healthy adults tends to increase with age, primarily affecting the outer macular regions, while sparing the central millimeter ETDRS subfield. The retromode imaging modality provided superior detection of DLDs specifically at the posterior pole, allowing the visualization and quantification of alterations that would otherwise remain undetectable with conventional color FP. These data further support the benefits derived from this innovative noninvasive imaging technology that should be considered for future multimodal imaging-based AMD classifications. A similar approach in a wider range of populations would better define the aging process affecting retinal physiology before the beginning of the pathologic process.

Acknowledgments

The authors thank Riccardo Ferraris de Gaspare (Nidek, Gamagori, Japan) for the technical support.

Footnotes and Disclosures

Originally received: March 8, 2023.
Final revision: June 17, 2023.
Accepted: July 13, 2023.
Available online: July 19, 2023. Manuscript no. ORET-D-23-00131R1.

[1] Eye Clinic, Department of Biomedical and Clinical Science, University of Milan, Milan, Italy.

[2] The University of Sydney, Save Sight Institute, Discipline of Ophthalmology, Sydney Medical School, Sydney, NSW, Australia.

Presented at the Association for Research in Vision and Opthalmology 2023 Meeting, New Orleans, LA.

Disclosure(s):

All authors have completed and submitted the ICMJE disclosures form.

The authors have made the following disclosures: M.C.: Financial support − Bayer, Nidek, Novartis, Zeiss, Heidelberg Engineering

A.I.: Consultant − Bayer, Novartis, Allergan; Financial support − Roche, Heidelberg Engineering

G.S.: Consultant − Heidelberg Engineering, CenterVue, Allergan, Bayer, Genetech, Novartis, Quantel Medical, Carl Zeiss Meditec, Appellis, Boheringer, Roche; Financial support − Optos, OptoVue, Topcon; Patent − Ocular Instruments

The other authors have no proprietary or commercial interest in any materials discussed in this article.

HUMAN SUBJECTS: Human subjects were included in this study. The study was approved by the Milano Area 1 institutional review board and was conducted in accordance with the tenets of the Declaration of Helsinki.

Written informed consent was obtained from all eligible participants at the time of enrollment.

No animal subjects were included in this study.

Author Contributions:

Conception and design: Cozzi, Monteduro, Airaldi, Parrulli, Staurenghi, Invernizzi

Data collection: Cozzi, Monteduro, Airaldi, Parrulli, Cinus, Trinco

Analysis and interpretation: Cozzi, Monteduro, Airaldi, Parrulli, Staurenghi, Invernizzi

Obtained funding: Study was performed as part of the authors' regular employment duties. No additional funding was provided.

Overall responsibility: Cozzi, Monteduro, Airaldi, Invernizzi

Abbreviations and acronyms:
AMD = age-related macular degeneration; **BCVA** = best-corrected visual acuity; **BM** = Bruch's membrane; **CI** = confidence interval; **D** = diopters; **DL** = deviated-left; **DLD** = drusen-like deposit; **DR** = deviated-right; **FP** = fundus photography; **GLMM** = generalized linear mixed-effects model; **ICC** = intraclass correlation coefficient; **IQR** = interquartile range; **RPE** = retinal pigment epithelium; **RR** = relative risk; **SD** = standard deviation; **SD-OCT** = spectral-domain OCT.

Keywords:
Aging, Color fundus photography, Confocal scanning laser ophthalmoscopy, Drusen, Drusen-like deposits, Retromode.

Correspondence:
Alessandro Invernizzi, Via GB Grassi 74, 20157 Milan, Italy. E-mail: alessandro.invernizzi@gmail.com.

References

1. Ardeljan D, Chan CC. Aging is not a disease: distinguishing age-related macular degeneration from aging. *Prog Retin Eye Res*. 2013;37:68−89.
2. Spaide RF, Curcio CA. Drusen characterization with multimodal imaging. *Retina*. 2010;30:1441−1454.
3. Age-Related Eye Disease Study Research Group. The age-related eye disease study (AREDS) system for classifying cataracts from photographs: AREDS report no. 4. *Am J Ophthalmol*. 2001;131:167−175.
4. Ferris FL, Wilkinson CP, Bird A, et al. Clinical classification of age-related macular degeneration. *Ophthalmology*. 2013;120:844−851.
5. Rudolf M, Clark ME, Chimento MF, et al. Prevalence and morphology of druse types in the macula and periphery of eyes with age-related maculopathy. *Invest Ophthalmol Vis Sci*. 2008;49:1200−1209.
6. Ramrattan RS, van der Schaft TL, Mooy CM, et al. Morphometric analysis of Bruch's membrane, the choriocapillaris, and the choroid in aging. *Invest Ophthalmol Vis Sci*. 1994;35:2857−2864.
7. Pauleikhoff D, Harper CA, Marshall J, Bird AC. Aging changes in Bruch's membrane. A histochemical and morphologic study. *Ophthalmology*. 1990;97:171−178.
8. Invernizzi A, Pellegrini M, Acquistapace A, et al. Normative data for retinal-layer thickness maps generated by spectral-

domain OCT in a White population. *Ophthalmol Retina*. 2018;2:808−815.e1.
9. Cozzi M, Monteduro D, Parrulli S, et al. Sensitivity and specificity of multimodal imaging in characterizing drusen. *Ophthalmol Retina*. 2020;4:987−995.
10. Corradetti G, Corvi F, Sadda SR. Subretinal drusenoid deposits revealed by color SLO and retro-mode imaging. *Ophthalmology*. 2021;128:409. https://doi.org/10.1016/j.ophtha.2020.09.038.
11. Mainster MA, Desmettre T, Querques G, et al. Scanning laser ophthalmoscopy retroillumination: applications and illusions. *Int J Retina Vitreous*. 2022;8:71. https://doi.org/10.1186/s40942-022-00421-0.
12. Acton JH, Cubbidge RP, King H, et al. Drusen detection in retro-mode imaging by a scanning laser ophthalmoscope. *Acta Ophthalmol*. 2011;89:e404−e411.
13. Diniz B, Ribeiro RM, Rodger DC, et al. Drusen detection by confocal aperture-modulated infrared scanning laser ophthalmoscopy. *Br J Ophthalmol*. 2013;97:285−290.14.
14. Curcio CA, Medeiros NE, Millican CL. Photoreceptor loss in age-related macular degeneration. *Invest Ophthalmol Vis Sci*. 1996;37:1236−1249.
15. Curcio CA, Owsley C, Jackson GR. Spare the rods, save the cones in aging and age-related maculopathy. *Invest Ophthalmol Vis Sci*. 2000;41:2015−2018.
16. Flamendorf J, Agrón E, Wong WT, et al. Impairments in dark adaptation are associated with age-related macular degeneration severity and reticular pseudodrusen. *Ophthalmology*. 2015;122:2053−2062.
17. Owsley C, McGwin G, Clark ME, et al. Delayed rod-mediated dark adaptation is a functional biomarker for incident early age-related macular degeneration. *Ophthalmology*. 2016;123:344−351.
18. Grewal MK, Chandra S, Bird A, et al. Scotopic thresholds on dark-adapted chromatic perimetry in healthy aging and age-related macular degeneration. *Sci Rep*. 2021;11:10349. https://doi.org/10.1038/s41598-021-89677-4.
19. Wang JJ, Rochtchina E, Lee AJ, et al. Ten-year incidence and progression of age-related maculopathy: the Blue Mountains Eye Study. *Ophthalmology*. 2007;114:92−98.
20. Joachim N, Mitchell P, Burlutsky G, et al. The incidence and progression of age-related macular degeneration over 15 years: the Blue Mountains Eye Study. *Ophthalmology*. 2015;122:2482−2489.
21. Waldstein SM, Vogl WD, Bogunovic H, et al. Characterization of drusen and hyperreflective foci as biomarkers for disease progression in age-related macular degeneration using artificial intelligence in optical coherence tomography. *JAMA Ophthalmol*. 2020;138:740−747.
22. Pollreisz A, Reiter GS, Bogunovic H, et al. Topographic distribution and progression of soft drusen volume in age-related macular degeneration implicate neurobiology of fovea. *Invest Ophthalmol Vis Sci*. 2021;62:26. https://doi.org/10.1167/iovs.62.2.26.
23. Saßmannshausen M, Behning C, Weinz J, et al. Characteristics and spatial distribution of structural features in age-related macular degeneration: a MACUSTAR study report. *Ophthalmol Retina*. 2023;7:420−430.
24. Bressler NM, Bressler SB, West SK, et al. The grading and prevalence of macular degeneration in Chesapeake Bay watermen. *Arch Ophthalmol*. 1989;107:847−852.
25. Sarks SH, Arnold JJ, Killingsworth MC, Sarks JP. Early drusen formation in the normal and aging eye and their relation to age related maculopathy: a clinicopathological study. *Br J Ophthalmol*. 1999;83:358−368.
26. Silvestri G, Williams MA, McAuley C, et al. Drusen prevalence and pigmentary changes in Caucasians aged 18-54 years. *Eye (Lond)*. 2012;26:1357−1362.
27. Klein R, Klein BE, Linton KL. Prevalence of age-related maculopathy. The Beaver Dam Eye Study. *Ophthalmology*. 1992;99:933−943.
28. Pedersen HR, Gilson SJ, Dubra A, et al. Multimodal imaging of small hard retinal drusen in young healthy adults. *Br J Ophthalmol*. 2018;102:146−152.
29. Munch IC, Li XQ, Ahmad SSM, et al. Small hard macular drusen and associations in 11- to 12-year-old children in the Copenhagen Child Cohort 2000 Eye Study. *Invest Ophthalmol Vis Sci*. 2019;60:1454−1460.
30. Spooner K, Phan L, Cozzi M, et al. Comparison between two multimodal imaging platforms: Nidek Mirante and Heidelberg Spectralis. *Graefes Arch Clin Exp Ophthalmol*. 2021;259:1791−1802.
31. Spaide RF, Caujolle S, Otto T. Intermediate and deep capillary plexuses in machine learning segmentation of high-resolution optical coherence tomography imaging. *Retina*. 2021;41:1314−1317.
32. Spaide RF, Otto T, Caujolle S, et al. Lateral resolution of a commercial optical coherence tomography instrument. *Transl Vis Sci Technol*. 2022;11:28.